

Test of QEDPS: A Monte Carlo for the hard photon distributions in e^+e^- annihilation process

Y. Kurihara, J. Fujimoto, T. Munehisa(*) and Y. Shimizu

National Laboratory for High Energy Physics(KEK)

Oho 1-1 Tsukuba, Ibaraki 305, Japan

(*)Faculty of Engineering, Yamanashi University

Takeda, Kofu, Yamanashi 400, Japan

ABSTRACT

The validity of a photon shower generator QEDPS has been examined in detail. This is formulated based on the leading-logarithmic renormalization equation for the electron structure function and it provides a photon shower along the initial e^\pm . The main interest in the present work is to test the reliability of the generator to describe a process accompanying hard photons which are detected. For this purpose, by taking the HZ^0 production as the basic reaction, the total cross section and some distributions of the hard photons are compared between two cases that these photons come from either those generated by QEDPS or the hard process $e^+e^- \rightarrow HZ^0\gamma\cdots\gamma$. The comparison performed for the single and the double hard photon has shown a satisfactory agreement which demonstrated that the model is self-consistent.

1 Introduction

In a series of works[1]-[3] we have proposed a generator QEDPS which develops a photon shower along the initial e^\pm of any hard annihilation process. This gives the correction by the initial state radiation(ISR). Usually ISR is implemented by the structure function of the initial e^\pm . By using the generator, however, it is possible not only to give the corrected total cross section with arbitrary cuts but also a distribution over any kinematical variable including transverse momentum of photons. It should be also noticed that the annihilating e^+ and e^- no more make the head-on collision, as they deviate from the beam axis by the radiation.

In the following sections we examine in detail the validity of QEDPS. We take $e^+e^- \rightarrow HZ^0$ together with possible hard photons as the hard process. The next section will make a brief review of QEDPS. We also summarize the analytic form of the structure function up to $O(\alpha^2)$, which should be compared against the photon shower in section 3. Section 4 is devoted to the numerical test of QEDPS. The correction to the total cross section is tested in the sub section 4.1 between the simulation and the analytic structure function. The subsequent two sub sections, 4.2 and 4.3, are devoted to a single and double hard photon emission, respectively. The last section gives the summary and discussions.

2 QEDPS

We review briefly the formulation of QEDPS in this section. The basic assumption is that the structure function of an electron, with the virtuality Q^2 and the momentum fraction x , obeys the Altarelli-Parisi equation

$$\frac{dD(x, Q^2)}{d \ln Q^2} = \frac{\alpha}{2\pi} \int_x^1 \frac{dy}{y} P_+(x/y) D(y, Q^2), \quad (1)$$

in the leading-log(LL) approximation[4]. To solve this we modify the split-function as follows;

$$P_+(x) \simeq \theta(1 - \epsilon - x)P(x) - \delta(1 - x) \int_0^{1-\epsilon} dy P(x), \quad P(x) = \frac{1+x^2}{1-x}. \quad (2)$$

Here ϵ is a small quantity specified later. Then the original equation can be converted to the integral equation.

$$D(x, Q^2) = \Pi(Q^2, Q_s^2) D(x, Q_s^2) + \frac{\alpha}{2\pi} \int_{Q_s^2}^{Q^2} \frac{dK^2}{K^2} \Pi(Q^2, K^2) \int_x^{1-\epsilon} \frac{dy}{y} P(y) D(x/y, K^2). \quad (3)$$

Here, rigorously speaking, Q_s^2 should be m_e^2 as it gives the initial condition. For simplicity the fine structure constant α is assumed not running with Q^2 . The function Π , which is nothing but the Sudakov factor, is given by

$$\Pi(Q^2, Q'^2) = \exp \left(-\frac{\alpha}{2\pi} \int_{Q'^2}^{Q^2} \frac{dK^2}{K^2} \int_0^{1-\epsilon} dx P(x) \right), \quad (4)$$

and implies the probability that the electron evolves from Q'^2 to Q^2 without emitting hard photon. In other words Π already contains the contributions from the soft photon emission, which causes the change of the electron virtuality, and from the loop corrections in all orders of perturbation.

The integral form Eq.(3) can be solved by iterating the right-hand side in a successive way. Then it is apparent that the emission of n photons corresponds to the n -th iteration. Hence it is possible to regard the process as a stochastic one that suggests the following algorithm of the photon shower[1].

(a) Set $x_b = 1$. The variable x_b is the fraction of the light-cone momentum of the virtual electron that annihilates.

(b) Choose a random number η . If it is smaller than $\Pi(Q^2, Q_s^2)$, then the evolution stops. If not, one finds the virtuality K^2 that satisfies $\eta = \Pi(K^2, Q_s^2)$ with which a branching takes place.

(c) Fix x according to the probability $P(x)$ between 0 and $1 - \epsilon$. Then x_b is replaced by $x_b x$. One should go to (b) by substituting K^2 into Q_s^2 and repeat until it stops.

Once an exclusive process is fixed by this algorithm, each branching of a photon in the process is dealt with as a true process, that is, an electron with x, K^2 decays as

$$e^-(x, -K^2) \rightarrow e^-(xy, -K'^2) + \gamma(x(1-y), Q_0^2). \quad (5)$$

In the infinite momentum frame where the parent has the momentum $p = (E, \mathbf{0}_T, p_z)$, $E = \sqrt{p_z^2 - K^2}$, $p_z = xp^*$, the daughter electron and the photon have $p' = (E', \mathbf{k}_T, yp_z)$ and $k = (k_0, -\mathbf{k}_T, (1-y)p_z)$, respectively, with $E' = \sqrt{y^2 p_z^2 + \mathbf{k}_T^2 - K'^2}$ and $k_0 = \sqrt{(1-y)^2 p_z^2 + \mathbf{k}_T^2 + Q_0^2}$. Here we have introduced a cutoff Q_0^2 to avoid the infrared divergence. The momentum conservation at the branching gives

$$-K^2 = -K'^2/y + Q_0^2/(1-y) + \mathbf{k}_T^2/(y(1-y)), \quad (6)$$

which in turn determines \mathbf{k}_T^2 from y, K^2, K'^2 . Hence one can get the information on the transverse momentum. This enables us to give the \mathbf{k}_T^2 distribution by the simulation as well as the shape of x .

Further the kinematical boundary $y(K^2 + Q_0^2/(1-y)) \leq K'^2$, equivalent to $\mathbf{k}_T^2 > 0$, fixes ϵ as

$$\epsilon = Q_0^2/K'^2, \quad (7)$$

since $K^2 \ll K'^2$ is expected. In ref.[3] it has been demonstrated that the existence of ϵ which depends on the virtuality gives rise to a small but non-negligible contribution to the structure function, though it is a constant. This is because when the virtuality becomes to the order of Q_0^2 , ϵ is not small, while in Eq.(3) it is assumed to be small enough.

The above description of the algorithm has shown the single cascade scheme. This implies that either of e^- or e^+ is able to radiate photons when the axial gauge vector is chosen along the momentum of the other electron, namely e^+ or e^- . In writing a computer code for the shower, however, it is convenient to use the double cascade scheme to ensure the symmetry of the radiation between e^+ and e^- [5]. It can be shown that these two are mathematically equivalent in the LL approximation. The extra finite contribution due to ϵ is, however, different between single and double cascade scheme. The details will be found in ref.[3].

In the formulation there are two parameters Q_s^2 and Q_0^2 . In the program the following values are chosen:

$$Q_s^2 = m_e^2 e = m_e^2 \times 2.71828 \dots, \quad Q_0^2 = 10^{-12} \text{ GeV}^2. \quad (8)$$

The former value was settled to take into account effectively the constant term -1 of β in such a way $\beta = (2\alpha/\pi)(\ln(s/m_e^2) - 1) = (2\alpha/\pi) \ln(s/(m_e^2 e))$. Since the second parameter is unphysical, any physical observable should not depend on it. It has been checked that increasing Q_0^2 up to $O(m_e^2/10)$ leaves the result unchanged in the statistical error of the event generation.

3 Structure function

The differential equation Eq.(1) can be easily solved if one introduces the moment of the structure function by[8]

$$D(n, s) = \int_0^1 dx x^{n-1} D(x, s). \quad (9)$$

The solution is then

$$D(n, s) = \exp \left[\frac{\beta}{2} \left(\frac{3}{2} - 2S_1(n-1) - \frac{1}{n} - \frac{1}{n+1} \right) \right], \quad (10)$$

with the initial condition $D(x, Q_s^2) = \delta(1-x)$. Here

$$S_1(n) = \sum_{j=1}^{\infty} \frac{n}{j(j+n)}. \quad (11)$$

is an analytic continuation of the finite sum $\sum_{j=1}^n 1/j$ into the complex n -plane. We expand Eq.(10) with respect to β in the following way

$$\begin{aligned} D(n, s) \simeq & \left(1 + \frac{3}{8}\beta + \frac{9}{128}\beta^2 \right) \exp \left(-\frac{\beta}{2} S_1(n-1) \right) \\ & - \frac{\beta}{4} \left(\frac{1}{n} + \frac{1}{n+1} \right) \left(1 - \frac{\beta}{2} S_1(n-1) \right) - \left(\frac{\beta}{4} \right)^2 \frac{3}{2} \left(\frac{1}{n} + \frac{1}{n+1} \right) \\ & + \left(\frac{\beta}{4} \right)^2 \frac{1}{2} \left(\frac{1}{n} + \frac{1}{n+1} \right)^2, \end{aligned} \quad (12)$$

and further for $n \rightarrow \infty$

$$\exp \left(-\frac{\beta}{2} S_1(n-1) \right) \simeq \exp \left(-\frac{\beta}{2} (\gamma_E + \ln n) \right) - \frac{\beta}{2} [S_1(n-1) - \gamma_E - \ln n]$$

$$+\frac{1}{2!}\left(\frac{\beta}{2}\right)^2\{[S_1(n-1)]^2-(\gamma_E+\ln n)^2\}, \quad (13)$$

where $\gamma_E = 0.57721 \dots$ is the Euler's constant. The inverse transformation defined by

$$D(x, s) = \int_{c-i\infty}^{c+i\infty} \frac{dn}{2\pi i} x^{-n} D(n, s), \quad (14)$$

with $c > 0$ being a real number to fix the integration path, gives

$$D(x, s) = \left[1 + \frac{3}{8}\beta + \left(\frac{9}{128} - \frac{\zeta(2)}{8}\right)\beta^2\right] \frac{\beta}{2}(1-x)^{\beta/2-1} - \frac{\beta}{4}(1+x) - \frac{\beta^2}{32}\left[4(1+x)\ln(1-x) + \frac{1+3x^2}{1-x}\ln x + (5+x)\right], \quad (15)$$

Here we have made a resummation to get the first term $(1-x)^{\beta/2-1}$.

Eq.(15) is used throughout for the test of QEDPS in the following sections. One should keep in mind that these results are obtained in the leading-log(LL) approximation and non-leading terms are not fully included corresponding to QEDPS.

4 Numerical test of QEDPS

4.1 Corrected total cross section

In Ref.[1] we have already compared the model with the analytic structure function[6] and also with the perturbative calculations of the initial state radiation(ISR) available up to $O(\alpha^2)$ [8]. In these comparisons we had obtained a satisfactory agreement, but as explained in section 1 the recovery of the missing finite term should give better agreement. This is important to be confirmed since the experimental accuracy is becoming less than 1%.

The basic hard process is

$$e^+e^- \rightarrow HZ^0. \quad (16)$$

We take this reaction as our example since it is not only the most suitable one to test the ISR corrections as there is no final state radiation but also very simple process

with a few Feynman diagrams even when some extra photons are attached. Its cross section $\sigma_0(s)$ is combined with QEDPS to generate the events with indefinite number of photons. None of them is assumed to be observed, that is, no cut is imposed on the photons. On the other hand the corrected total cross section can be easily estimated by convoluting $\sigma_0(s)$ with the structure function. In this work all the hard process is calculated by Monte Carlo integration[7]. In other words we also have a generator for the hard process.

In Table 1 we show the results evaluated by these two different methods. The used parameters are given by

$$\begin{aligned}\alpha &= 1/137.036, \quad m_e = 0.511 \times 10^{-3} \text{ GeV}, \\ M_W &= 80.230 \text{ GeV}, \quad M_Z = 91.188 \text{ GeV}.\end{aligned}\tag{17}$$

The mass of Higgs particle is taken to be the same as M_W . This has no realistic meaning. The total energy is chosen in the range $\sqrt{s} = 200 - 1000 \text{ GeV}$, roughly from LEP200 to linear colliders. From the table one finds that the simulation agrees well with the analytic formula within the accuracy less than 0.4%. This indicates that QEDPS effectively reproduces the structure function which includes the soft photon resummation and also the expansion of terms up to $O(\beta^2)$.

| $\sqrt{s}(\text{GeV})$ | HZ/ps | HZ/sf | $(HZ/\text{ps})/(HZ/\text{sf})-1$ |
|------------------------|------------------------------------|------------------------------------|-----------------------------------|
| 200 | $(5.727 \pm 0.004) \times 10^{-1}$ | $(5.727 \pm 0.002) \times 10^{-1}$ | 0.0% |
| 300 | $(2.411 \pm 0.002) \times 10^{-1}$ | $(2.419 \pm 0.001) \times 10^{-1}$ | -0.33% |
| 400 | $(1.193 \pm 0.002) \times 10^{-1}$ | $(1.196 \pm 0.001) \times 10^{-1}$ | -0.25% |
| 500 | $(7.125 \pm 0.007) \times 10^{-2}$ | $(7.137 \pm 0.003) \times 10^{-2}$ | -0.17% |

Table 1 Total cross sections(pb) without cut.

Finally we compare QEDPS with the fixed order perturbative calculations for the higher order corrections. At $\sqrt{s} = 500 \text{ GeV}$, for example, the total cross sections are $\sigma_0 = 5.766 \times 10^{-2} \text{ pb}$ in the tree level(Eq.(16)), $\sigma_1 = 7.181 \times 10^{-2} \text{ pb}$ for the corrected one up to $O(\alpha)$ and $\sigma_2 = 7.208 \times 10^{-2} \text{ pb}$ up to $O(\alpha^2)$ [8, 10], respectively. The

numbers in Table 1 do not include the so called K -factor ($K = 1 + \alpha/\pi(\pi^2/3 - 1/2) = 1.00648\dots$) which recovers almost the constant term in $O(\alpha)$. Multiplying this value, we get 7.171×10^{-2} pb of HZ/ps or 7.183×10^{-2} pb of HZ/sf , thus the convergence of the perturbation series shows a good behavior.

4.2 Single hard photon test

Let us consider the following experimental situation. Together with H and Z^0 we shall observe a hard photon with $E_\gamma > 1$ GeV outside of the cone of 5° from the beam axis. Inside the cone any number of photons can be radiated. The photons with $E_\gamma < 1$ GeV are regarded as soft and get no angular limitation. Hence one detects $HZ^0\gamma$ as the final state.

To estimate the total cross section and distributions with respect to some kinematical variables, which we specify later, we consider four different ways to estimate this cross section. The first one is simply to calculate it in the tree level

$$e^+e^- \rightarrow HZ^0\gamma. \quad (18)$$

Obviously this gives the lowest order result without any radiative correction. It is not expected to be precise enough then, but we include this result in our comparison.

The second one is the same process but corrected up to $O(\alpha)$ in perturbation, which should give more accurate estimation. In this case one has to evaluate the cross section for the process

$$e^+e^- \rightarrow HZ^0\gamma\gamma, \quad (19)$$

in the tree level under the experimental condition on the photons as same as before. Also one needs the one-loop correction to the process Eq.(18). All the necessary calculations are found in Ref.[8].

The third way is to impose the condition on the photons generated by QEDPS being combined with $d\sigma_0(s)$. This is the same thing as given in the previous section

but with the cut. We denote this estimation as $HZ/\gamma\text{ps}$ to imply that QEDPS is applied to the bare process Eq.(16) but one of the generated photons is observed.

The last one is to dress the photon shower to the radiative process Eq.(18) in the tree level. In this case the photon associated with HZ^0 production is regarded as the observed one. Other photons supplied by the simulation are supposed to be invisible so that they escape inside of the cone or are soft. We denote this process as $HZ\gamma/\text{ps}$. Here it is important not to make double counting of the hard photon. This can be achieved by the following manner. In Eq.(5) the virtuality of the initial e^\pm is required to satisfy $K^2 < K'^2$ at each branching in the cascade. This order should be also maintained for the electron in the process Eq.(18). In other words the virtuality of e^\pm in the cascade is restricted to be smaller than that appears in the hard process.

One should notice that the comparison of the third and the fourth cases provides a self-consistency check of the model while the first two allows the comparison with the perturbative calculations.

The results of the total cross sections are summarized in Table 2 which are obtained by these four different methods at various energies with the cut.

| $\sqrt{s}(\text{GeV})$ | $HZ\gamma$ (tree) | $HZ\gamma$ (up to $O(\alpha)$) | $HZ/\gamma\text{ps}$ | $HZ\gamma/\text{ps}$ |
|------------------------|------------------------|---------------------------------|------------------------------------|------------------------------------|
| 200 | 5.602×10^{-2} | 4.418×10^{-2} | $(4.534 \pm 0.008) \times 10^{-2}$ | $(4.424 \pm 0.002) \times 10^{-2}$ |
| 300 | 3.284×10^{-2} | 3.018×10^{-2} | $(3.086 \pm 0.016) \times 10^{-2}$ | $(2.945 \pm 0.002) \times 10^{-2}$ |
| 400 | 1.765×10^{-2} | 1.701×10^{-2} | $(1.754 \pm 0.010) \times 10^{-2}$ | $(1.648 \pm 0.001) \times 10^{-2}$ |
| 500 | 1.101×10^{-2} | 1.088×10^{-2} | $(1.143 \pm 0.007) \times 10^{-2}$ | $(1.048 \pm 0.001) \times 10^{-2}$ |

Table 2 Total cross sections(pb) : single-hard photon required.

At 500 GeV, the effect of $O(\alpha)$ corrections is small, less than 1%. It does not mean, however, that Born approximation is enough because the various distributions are different between them as shown in Fig.1. The plots show the first case and the histograms does the second one. Q is the virtuality of the s -channel virtual

boson(Z^0) or the invariant mass of the HZ^0 system. Q_z is the longitudinal momenta of this system. E^γ and E_t^γ are the energy and the transverse momentum of the required hard photon with respect to the beam axis, respectively. There is seen a large discrepancy in the Q and Q_z distributions. This is not surprising because there is no correction from the soft photon emission in the tree level case. On the other hand, E^γ and E_t^γ distributions agrees rather well.

Next we show in Fig.2 the comparison of the same distributions between the third case, HZ/γ ps and the second case, $HZ\gamma$ with the $O(\alpha)$ corrections. Here, again, the histograms show the second case and the plots the third one. This time Q and Q_z distribution are quite consistent because the both cases include the soft photon emission. In E^γ and E_t^γ distributions the third case shows an enhancement against to the second, but still consistent. One reason of this enhancement is presumably attributed to the fact that the constant terms of $O(\alpha/\pi)$ are missing in the LL approximation. Because of this enhancement, the total cross section of HZ/γ ps are always larger than that for $HZ\gamma$ with the $O(\alpha)$ corrections. QEDPS model, however, gives the events with the accuracy in the level of a few percent even though a hard photon is required.

Fig.3 shows the same comparison as in Figs.1 and 2 but between the fourth case, $HZ\gamma/\gamma$ ps, given by the plots and the second, $HZ\gamma$ with $O(\alpha)$ corrections, by the histograms. The agreement of all the distributions is very well. But the total cross sections in Table 2 of the fourth case are always smaller than the second one. This corresponds to the fact that in the lowest edge of the E_t^γ , the differential cross section of the fourth case is smaller than the second one. As mentioned above, we require the order of the virtuality to combine the one photon emission process with the QEDPS model. This recipe may be still naive and has some ambiguity in the very small E_t^γ region. On the other hand, in the large E_t^γ region, it works well. As long as one intends to study the events with a hard photon, the fourth is the best one.

From these results one can conclude that QEDPS is consistent not only with the

result of perturbation calculation up to the $O(\alpha)$ corrections but also within itself. This is a strong support for the reliability of QEDPS.

What happens if one convolutes the structure function with the radiative process Eq.(18), that is, $HZ\gamma/\text{sf}$? It is obvious that one has the double-counting because the hard photon is also contained in the structure function. Hence a naive convolution leads to an overestimation and one should introduce some special prescription to get a correct result[11].

It would be, however, interesting to see if QEDPS could reproduce the naive $HZ\gamma/\text{sf}$. In the former, as explained in the previous section, the virtuality cut prevents the double-counting. Then one may expect that to remove this cut would give the same result as $HZ\gamma/\text{sf}$. One kinematical difference should be noticed. In the case of the structure function the head-on collision of e^\pm takes place. On the other hand, with QEDPS the annihilation of electrons in the hard process cannot make the head-on collision because an emitted photon has a finite p_t^γ . To compare these two on the same ground then, we require the hard photon cut in *the CM system of the annihilating e^\pm* . The results summarized in Table 3 show that the above consideration is legitimate. The total cross section in the first row calculated by the structure function does not show any significant difference between Lab. and CM system while that by QEDPS in the second row considerably changes, resulting the consistent number with $HZ\gamma/\text{sf}$ only where the cut is imposed in the CM system. These results are unphysical after all, as the double-counting is allowed and the cut in the CM system is artificial. The comparison, however, provides another evidence that QEDPS is consistent with the structure function.

| hard photon cut | in Lab. sys. | in CM sys. |
|--|------------------------------------|------------------------------------|
| $\sigma(HZ\gamma/\text{sf})$ | $(1.256 \pm 0.002) \times 10^{-2}$ | $(1.266 \pm 0.001) \times 10^{-2}$ |
| $\sigma(HZ\gamma/\text{ps})$ without the virtuality cut | $(1.415 \pm 0.005) \times 10^{-2}$ | $(1.260 \pm 0.001) \times 10^{-2}$ |

Table 3 Total cross sections(pb) at $\sqrt{s}=500\text{GeV}$: single-hard photon required.

4.3 Double hard photon test

Further check of the model is possible by requiring the double hard photon emission. In this case, however, the perturbative calculation is restricted to only the tree process, Eq.(19), as we have no loop-correction of $O(\alpha^3)$ yet. Hence the first estimation comes from this tree process.

The second one is to dress the photon shower to the process Eq.(16) in the similar way as the third case in the previous section, It means that the two hard photons are generated by QEDPS.

The third one is to apply QEDPS to the process Eq.(19). In this case, two hard photons originate from the hard process Eq.(19) and others from the simulation are not observed.

The cuts for the hard photon is the same as before. Table 4 shows that even though the double-photon is required, QEDPS works in a consistent way independent of the allocation of the hard photon.

| $\sqrt{s}(\text{GeV})$ | $HZ\gamma\gamma$ | $HZ/\gamma\gamma\text{ps}$ | $HZ\gamma\gamma/\text{ps}$ |
|------------------------|--------------------------------|--------------------------------|--------------------------------|
| 200 | $(2.120\pm0.004)\times10^{-3}$ | $(1.644\pm0.018)\times10^{-3}$ | $(1.640\pm0.003)\times10^{-3}$ |
| 300 | $(2.161\pm0.004)\times10^{-3}$ | $(2.040\pm0.017)\times10^{-3}$ | $(1.922\pm0.004)\times10^{-3}$ |
| 400 | $(1.384\pm0.003)\times10^{-3}$ | $(1.370\pm0.011)\times10^{-3}$ | $(1.257\pm0.003)\times10^{-3}$ |
| 500 | $(9.481\pm0.014)\times10^{-4}$ | $(9.883\pm0.062)\times10^{-4}$ | $(8.707\pm0.022)\times10^{-4}$ |

Table 4 Total cross sections(pb) : double-hard photon required.

Fig.4 shows the comparison in the distributions. In this figure, the histograms are for $HZ/\gamma\gamma(\text{tree})$ and the cross and the circle correspond to $HZ/\gamma\gamma\text{ps}$ and $HZ\gamma\gamma/\text{ps}$, respectively. There appears a discrepancy in the distributions of Q and Q_z between the Born and the other two with QEDPS because the higher order corrections are missing in the first case. On the other hand, in the region of high Q , $HZ/\gamma\gamma\text{ps}$ and $HZ\gamma\gamma/\text{ps}$ are quite consistent. In the low region of Q , however, there seems a difference. Since there is no perturbative calculation with higher order we cannot say definitely which distribution is better but it is known in the study of QCD parton shower that the LL approximation always gives bigger estimation than the exact

one at larger momentum transfer region. E^γ and E_t^γ distributions agree well among three cases. As a conclusion, these results show the self-consistency of the QEDPS model again even for the double hard photons.

5 Summary and discussions

In this work we have tested QEDPS, a generator for the radiative corrections in e^+e^- annihilation. The total cross section corrected by QEDPS agrees with that calculated by the analytic formula of the structure function with the accuracy less than around 0.3% in the energy range of LEP200 to linear colliders. We checked the hard photon distribution of QEDPS against the calculation of the matrix element with the $O(\alpha)$ corrections and got an agreement. In order to make the self-consistency check, we applied QEDPS not only to $e^+e^- \rightarrow HZ^0$ but also to $e^+e^- \rightarrow HZ^0\gamma$ and $HZ^0\gamma\gamma$. In these cases we have introduced the virtuality cut to avoid the double-counting of the hard photon. As the result it has been shown that QEDPS is self-consistent in various distributions. Through all of these studies we conclude that the model for the photon showers for the ISR is established fairly well even in the LL approximation. This is also demonstrated for more complicated process such as $e^+e^- \rightarrow \mu^-\nu_\mu u\bar{d}$ as described in Ref.[13].

In the present work we have restricted the radiation only to ISR. The extension to include the final state radiation(FSR) is straightforward. In this case, however, a problem emerges how to incorporate with the interference between ISR and FSR, which is, in general, not so small to be ignored safely. Also the extension to the next-to-leading-logarithm(NLL) is urgent to make more precise predictions. This can be done in the same way as that in QCD parton shower[14]. These problems are now under investigation.

Acknowledgements

We would like to thank our colleagues of KEK working group(Minami-Tateya) and those in LAPP for valuable discussions. Particularly we are indebted to F. Boudjema, G. Coignet, T. Kaneko and D. Perret-Gallix for their continuous interest and encouragement. This work has been done under the collaboration between KEK and LAPP supported by Monbusho, Japan(No. 07044097) and CNRS/IN2P3, France.

References

- [1] J. Fujimoto, Y. Shimizu and T. Munehisa, Prog. Theor. Phys. **90**(1993)177.
- [2] J. Fujimoto, Y. Shimizu and T. Munehisa, Prog. Theor. Phys. **91**(1994)333.
- [3] T. Munehisa, J. Fujimoto, Y. Kurihara and Y. Shimizu, KEK CP-034, KEK Preprint 95-114, 1995.
- [4] R. Odorico, Nucl. Phys. **B172**(1980)157,
G. Marchesini and B.R. Webber, Nucl. Phys. **B238**(1984)1.
- [5] K. Kato and T. Munehisa, Phys. Rev. **D39**(1989)156.
- [6] V.N. Gribov and L.N. Lipatov, Sov. J. Nucl. Phys. **15**(1972)438,
E.A. Kuraev and V.S. Fadin, Sov. J. Nucl. Phys. **41**(1985)466; DESY Internal report L-Trans-297,1985,
J.P. Alexander, G. Bonvicini, P.S. Drell and R. Frey, Phys. Rev. **D37**(1988),56,
O. Nicrosini and L. Trentadue, Phys. Lett. **231B**(1989)487.
See also Chapter 11 of the first reference in [8].
- [7] S. Kawabata, Comput. Phys. Commun. **88**(1995)309.
- [8] J. Fujimoto et al., Progr. Theor. Phys. Suppl. **No.100**(1990)1,
J. Fujimoto, Y. Kurihara, Y. Shimizu, T. Munehisa and N. Nakazawa, in the *Proceedings of the Workshop on Physics and Experiments with Linear e^+e^- Collider*, Waikoloa, Hawaii, April, 1993.
- [9] M. Igarashi, *Proceedings of the Faculty of Science*, University of Tokai, vol.23, p.21, 1988.
- [10] F.A. Berends, W.L. van Neerven and G.J.H. Burgers, Nucl. Phys. **B297**(1988)429, Err. *ibid.* **B304**(1988)95.
- [11] G.J. van Oldenborgh, INLO-PUB-95/04, 1995, hep-ph/9503353.

- [12] A. Aeppli and D. Wyler, Phys. Lett. **B262**(1991)125,
G.J. van Oldenborgh, P.J. Franzini and A. Borrelli, Comput. Phys. Commun.
83(1994)14,
J. Fujimoto, T. Ishikawa, S. Kawabata, Y. Kurihara, D. Perret-Gallix and Y.
Shimizu, Nucl. Phys. Proc. Suppl. **37**(1994)169.
- [13] G. Altarelli, T. Sjostrand and F. Zwirner eds., "Physics at LEP2", CERN
Report 1996, to appear.
- [14] K. Kato and T. Muehisa, Phys. Rev. **D36**(1987)61,
K. Kato and T. Muehisa, Comput. Phys. Commun. **64**(1991)67,
K. Kato, T. Muehisa and H. Tanaka, Z. Phys. **C54**(1992)397.

Figure Captions

Fig.1 Comparison of the distributions between $HZ\gamma(\text{tree})$ and $HZ\gamma$ with up to the $O(\alpha)$ corrections at $\sqrt{s}=500\text{GeV}$. The plots show the former and the histograms the latter. Q and Q_z are the virtuality and the longitudinal momenta of the s -channel virtual boson, respectively. E^γ and E_t^γ are the energy and the transverse momentum of the required hard photon with respect to the beam axis, respectively.

Fig.2 Comparison of the distributions between $HZ\gamma$ with up to the $O(\alpha)$ corrections(histograms) and $HZ/\gamma\text{ps}$ (plots) at $\sqrt{s}=500\text{GeV}$.

Fig.3 Comparison of the distributions between $HZ\gamma$ with up to the $O(\alpha)$ corrections(histograms) and $HZ\gamma/\text{ps}$ (plots) at $\sqrt{s}=500\text{GeV}$.

Fig.4 Comparison of the distributions among $HZ\gamma\gamma$ (histogram), $HZ/\gamma\gamma\text{ps}$ (star plots) and $HZ\gamma\gamma/\text{ps}$ (circle plots) at $\sqrt{s}=500\text{GeV}$. The variables Q , Q_z , E^γ and E_t^γ are the same as in Fig. 1.

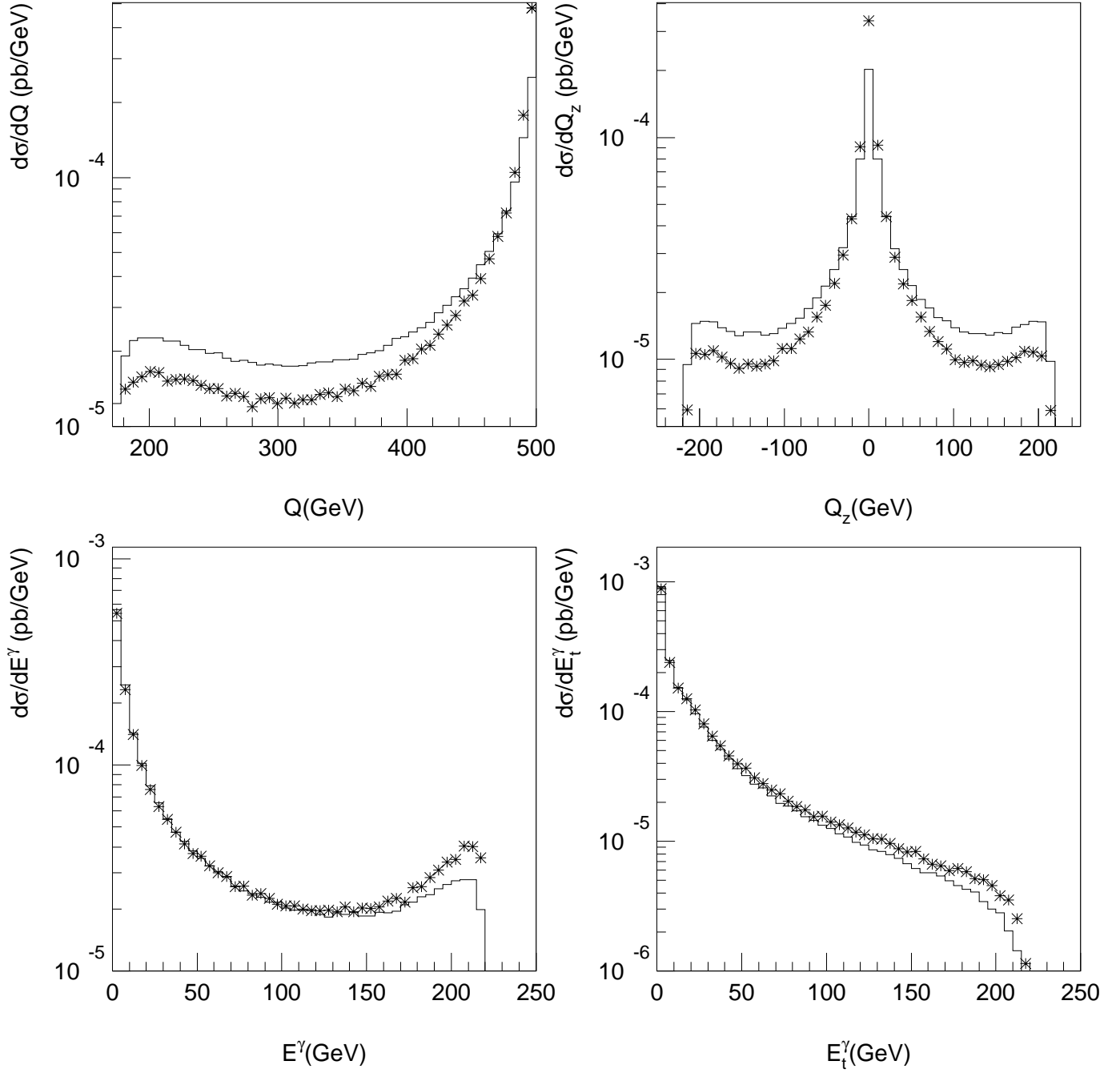


Figure 1:

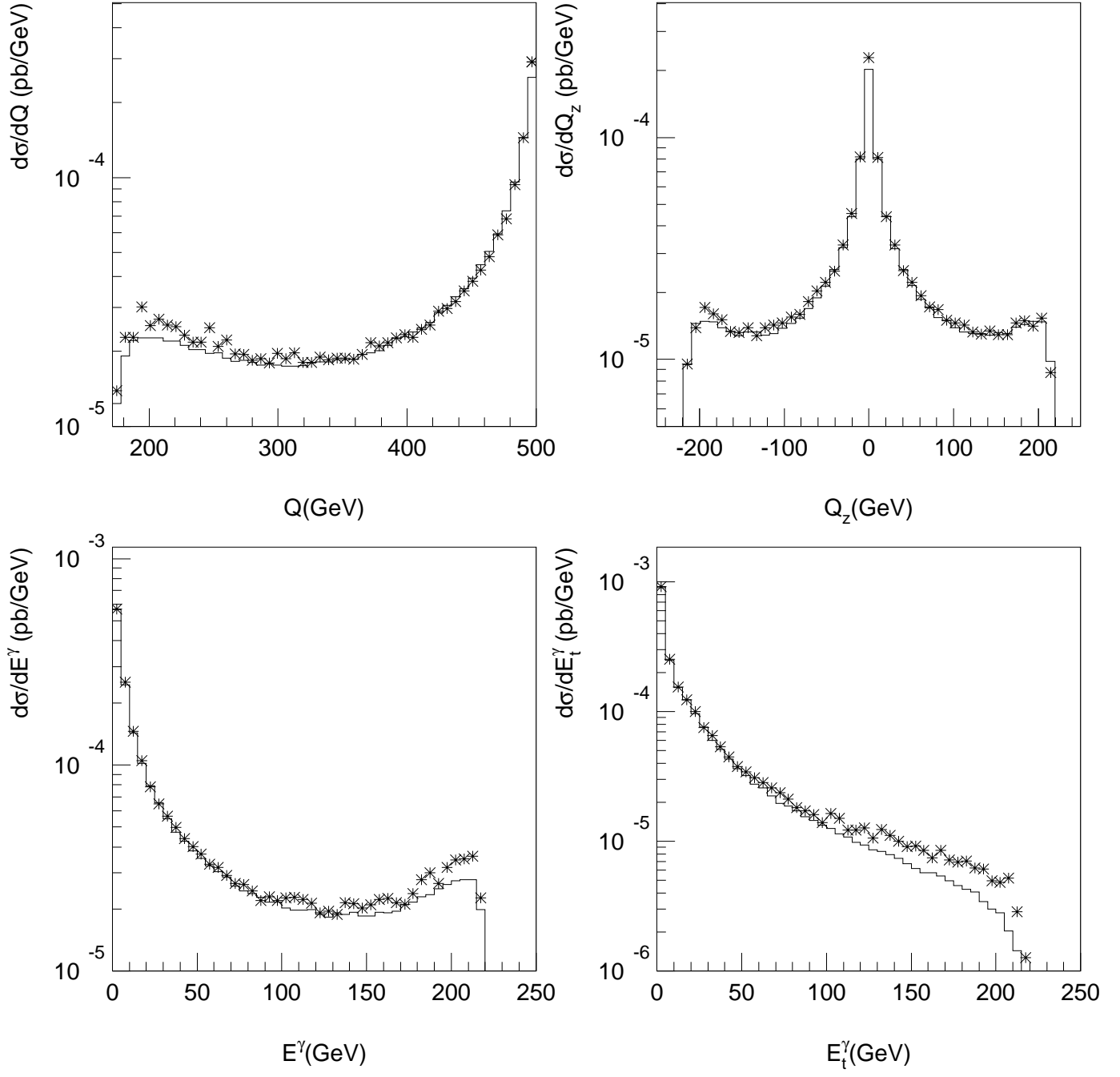


Figure 2:

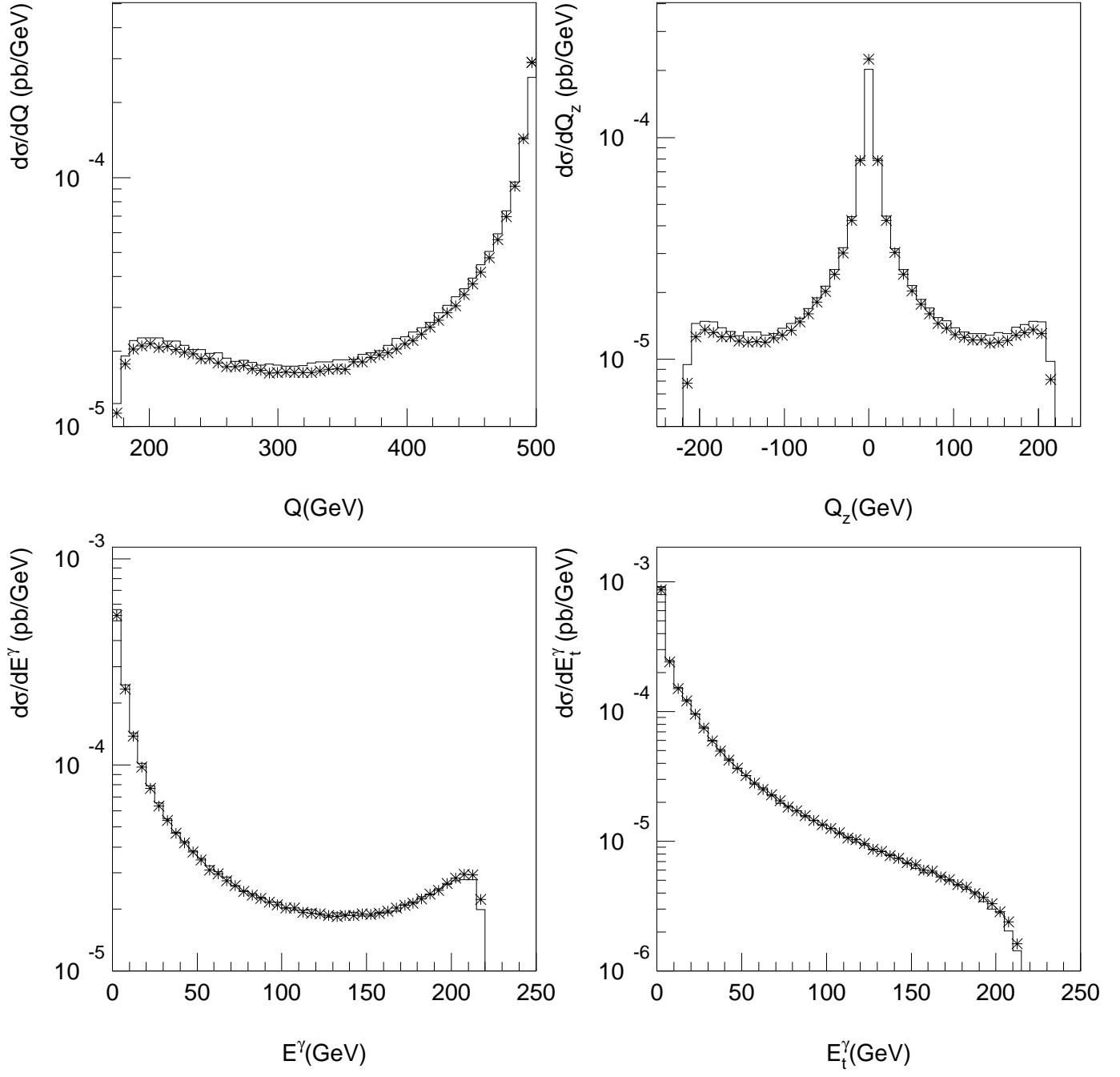


Figure 3:

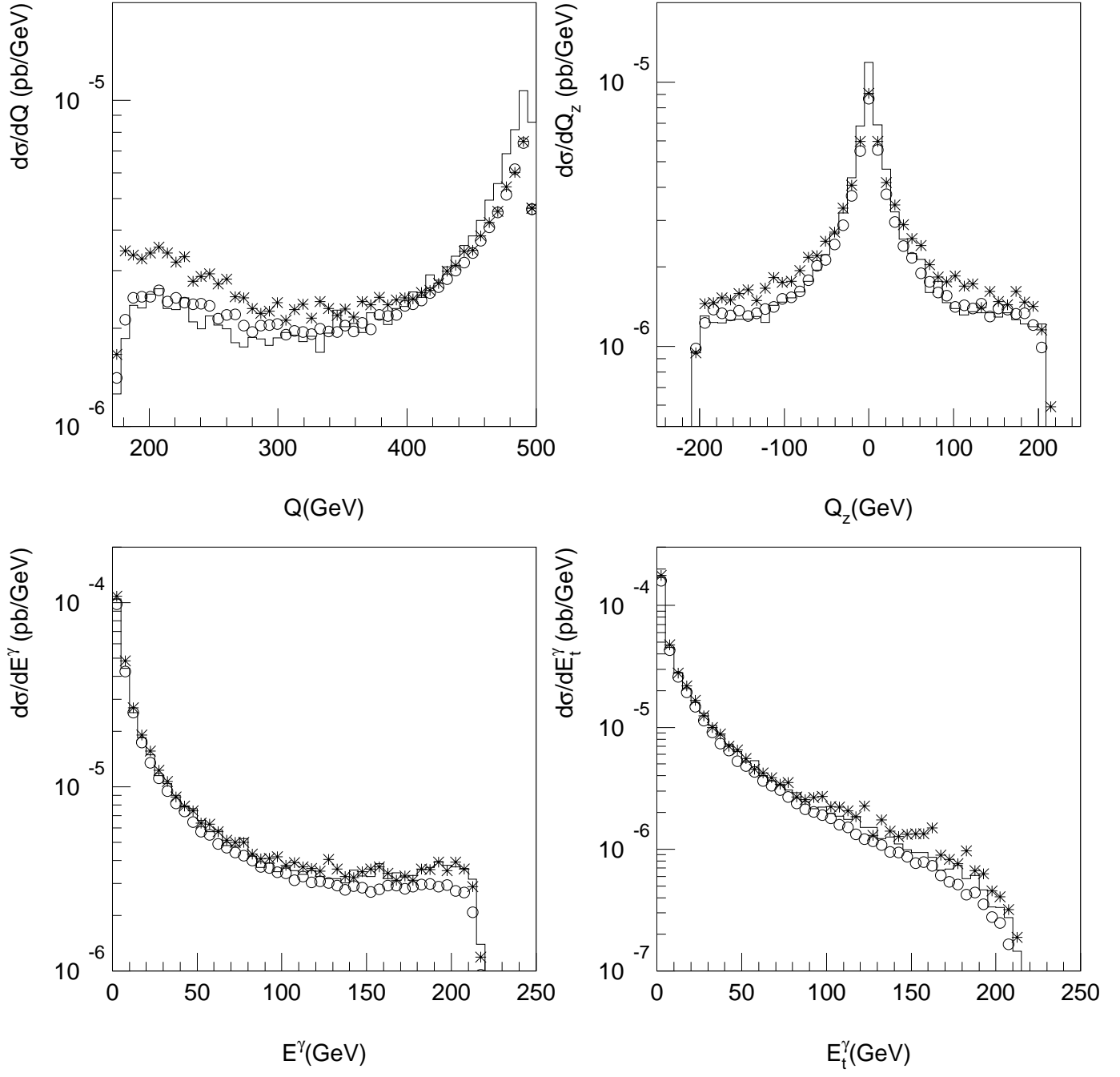


Figure 4: